Cell Reports
Article

High-Throughput Genetic Screen for Synaptogenic Factors: Identification of LRP6 as Critical for Excitatory Synapse Development

Kamal Sharma,[1] Se-Young Choi,[2] Yong Zhang,[1] Thomas J.F. Nieland,[3] Shunyou Long,[1] Min Li,[1] and Richard L. Huganir[1,*]
[1]Department of Neuroscience, Johns Hopkins University School of Medicine, 725 North Wolfe Street, Baltimore, MD 21205, USA
[2]Department of Physiology, Seoul National University School of Dentistry, Seoul 110-749, South Korea
[3]Stanley Center for Psychiatric Research, Broad Institute of Harvard and MIT, 7 Cambridge Center, Cambridge, MA 02142, USA
*Correspondence: rhuganir@jhmi.edu
http://dx.doi.org/10.1016/j.celrep.2013.11.008

SUMMARY

Genetic screens in invertebrates have discovered many synaptogenic genes and pathways. However, similar genetic studies have not been possible in mammals. We have optimized an automated high-throughput platform that employs automated liquid handling and imaging of primary mammalian neurons. Using this platform, we have screened 3,200 shRNAs targeting 800 proteins. One of the hits identified was LRP6, a coreceptor for canonical Wnt ligands. LRP6 regulates excitatory synaptogenesis and is selectively localized to excitatory synapses. In vivo knockdown of LRP6 leads to a reduction in the number of functional synapses. Moreover, we show that the canonical Wnt ligand, Wnt8A, promotes synaptogenesis via LRP6. These results provide a proof of principle for using a high-content approach to screen for synaptogenic factors in the mammalian nervous system and identify and characterize a Wnt ligand receptor complex that is critical for the development of functional synapses in vivo.

INTRODUCTION

Synaptogenesis is a highly specialized and complex phenomenon that involves precise target recognition by the pre- and postsynaptic machinery (McAllister, 2007; Okabe, 2012; Shen and Scheiffele, 2010; Siddiqui and Craig, 2011). Secreted ligands and cell surface molecules play key roles in the identification of the target and also initiate assembly of synaptic modules. Once a growth cone arrives in close proximity of its target site on the dendrite, a series of events act in an orchestrated fashion that includes assembly of macromolecular complexes required for signaling, adhesion, and neurotransmission (Chih et al., 2005; Dalva et al., 2000; Garner et al., 2000; Graf et al., 2004; Penzes et al., 2003; Scheiffele et al., 2000; Shen and Scheiffele, 2010; Williams et al., 2010). A rich repertoire of cell adhesion and signaling molecules allows for the construction of synapses with diverse structural and functional identities (O'Rourke et al., 2012). Molecular pathways that can selectively regulate the development of excitatory or inhibitory synapses fulfill the need for maintaining a dynamic balance between excitation and inhibition to ensure proper functioning of neuronal networks. Thus, it is of the utmost importance to identify the building blocks that define a synapse subtype. Moreover, the fact that many neurological disorders have been attributed to morphological defects at the synaptic level (Melom and Littleton, 2011; Mitchell, 2011) make it important to discover the genes that regulate the development and maturation of a wide array of synapse subtypes. However, despite a significant effort put into understanding synaptogenesis at the molecular level, master molecule(s) has remained elusive. In invertebrates, many genome-wide genetic screens have been carried out that led to the discovery of a handful of candidates involved in synapse development and maturation (Aberle et al., 2002; Featherstone et al., 2000; Kurusu et al., 2008; Schaefer et al., 2000). In the mammalian CNS, however, such screens have not been performed at a scale comparable to what has been possible in invertebrates. Biochemical approaches have proven useful in discovering some important genes involved in synaptogenesis at the neuromuscular junction such as Agrin and FGF-2, or Thrombospondin in retinal ganglion neurons (Allen et al., 2012; Christopherson et al., 2005; Nitkin et al., 1987; Peng et al., 1991), but such efforts have not had much success for synapses in the CNS. In recent years, a strategy of pooling and deconvoluting siRNA (Paradis et al., 2007) or ORF-cDNA clones has led to the discovery of novel synaptogenic proteins in the mammalian CNS (Linhoff et al., 2009; Takahashi et al., 2011).

Here, we adapted a high-content approach to develop a platform that can be employed in high-throughput screening for synaptogenic molecules using primary neuronal cultures. Employing automated high-content liquid handling and high-throughput image acquisition to screen several thousand shRNAs, we identified several factors, including LRP6, a coreceptor for Wnt ligands and signaling hub in canonical Wnt signaling (Pinson et al., 2000; Tamai et al., 2000; Wehrli et al., 2000), as a potential synaptogenic factor. Although the

importance of canonical Wnt signaling in the development of the neuromuscular junction in *Drosophila melanogaster* is well established (Koles and Budnik, 2012; Miech et al., 2008; Packard et al., 2002), the localization and function of any of the Wnt receptors at mammalian central synapses in vivo are unknown. Because Wnt receptors determine the nature of Wnt signaling triggered by a complex family of Wnt ligands (van Amerongen et al., 2008), knowledge of localization and function of Wnt receptors is critical. Hence, we carried out a detailed characterization of the role of LRP6 in central synapse formation. We show that LRP6 is exclusively localized to excitatory postsynaptic densities (PSDs) and is critical for synapse formation in vitro. In addition, we found that Wnt8A, a Wnt ligand that is predominantly expressed in forebrain, and is known to interact with LRP6, promotes excitatory synaptogenesis in vitro. Furthermore, we confirm that LRP6 is critical for the formation of functional excitatory synapses in vivo.

RESULTS

Optimization of shRNA High-Content Handling for Screening

To develop the high-throughput shRNA screen, we optimized automated culturing and immunolabeling using automated high-content liquid handling. A flowchart to outline the strategy is shown in Figure 1A where neurons were handled using a multidrop and robotic arm-assisted 96-well plate washing system. Once we optimized the cell density and the steps in robotic handling and image acquisition, we assessed the physiological health of neurons in a depolarization-induced CREB phosphorylation assay (Sheng et al., 1990). Neurons plated and handled in a high-content fashion were depolarized at 14 DIV with 50 mM KCl and probed with CREB and phospho-CREB antibodies. We found that neurons under such conditions robustly responded to depolarization, as evident by a significant increase in phospho-CREB signal in the nucleus indicating good physiological health (Figure 1B). Next, we tested the method for specificity and efficiency of immunolabeling of synaptic and somatodendritic markers. As shown in Figure 1C, immunolabeling with MAP-2, PSD95, and Gephyrin, well-characterized markers for somatodendritic regions, excitatory synapses, and inhibitory synapses, respectively, confirmed the morphological integrity of neurons as well as the specificity of acquired signals in automated handling and imaging.

With an optimized platform to carry out an assay using primary hippocampal neurons, we initiated a pilot shRNA screen to search for synaptogenic factors in the mammalian CNS. The Sigma-Aldrich MISSION shRNA Library available at the time of our initial screen offered four to five shRNAs for each target gene to enhance the possibility of efficient knockdown of a given target. However, a major limitation of the MISSION shRNA Library is that it did not have a reporter gene appropriate for assessing infection efficiency. The library employs a Puromycin selection marker that works on the principle of conferring resistance to infected neurons against the protein synthesis inhibitor Puromycin. For nonneuronal cells and for young neurons that are not extensively connected in a network, Puromycin works suitably, but once neurons are mature, activity in the network becomes critical for neuronal survival. In such a scenario, the death of even 50% of uninfected neurons will have adverse effects on the health of infected neurons despite Puromycin resistance. This makes Puromycin an unsuitable selection marker for mature neuronal networks. However, by assessing the effect of Puromycin on younger neurons, we found that the majority of the infected wells, when treated with Puromycin, showed a survival rate of more than 75% (Figure S1), suggesting a high probability of infection. We also tested a few sample shRNA clones to assess the potency of shRNA and efficiency of knockdown. As shown in an example in Figure S2, we observed a significant knockdown of Gephyrin by two out of five shRNA clones.

Next, we selected 800 transmembrane and secreted candidate proteins with four shRNAs against each (i.e., 3,200 shRNA clones) and designed a high-throughput screen to look for synaptogenic factors. Neurons were infected with lentiviral particles at 4 DIV, and fixed and immunostained at 13 DIV using the high-content handling methodology optimized earlier. Because there is currently no appropriate efficient automated image analysis tool that can carry out reliable quantitative analysis, we short-listed the hits by manual browsing of the wells. The wells that had a noticeably changed pattern for PSD95/Gephyrin staining were quantified in a low-throughput manner. Potential shRNA hits were subcloned into the pSuper plasmid that allows more efficient expression of shRNA. This was followed by secondary screening to address whether the shRNA clone can knock down its endogenous target and to assess the reproducibility of the primary screen.

To address the first question, we electroporated shRNA into dissociated hippocampal neurons, and 5 days postelectroporation and plating, lysed the neurons and probed for putative target protein. To address the second question, we transfected hippocampal neurons with shRNA in pSuper plasmid backbone along with GFP at 7 DIV and analyzed synapse number at 14 DIV. shRNAs that showed an effect on puncta number and knocked down their putative target protein were considered as positive hits. We describe here LRP6 as one of the hits that was discovered following this strategy and validated its role in the development of functional excitatory synapses (Figures 1 and 2).

LRP6 Regulates Excitatory Synapse Development

In the first round of the screen, wells infected with shRNA-lentiviral particles targeting LRP6 (shRNA-LRP6) showed a significant reduction in the number of PSD95 puncta, but no change in Gephyrin puncta (Figures 1D and 1E). shRNA-LRP6 significantly and specifically reduced endogenous LRP6 levels but had no effect on total PSD95 levels in hippocampal neurons. Next, we tested if knockdown of endogenous LRP6 led to a reduction in the number of morphological synapses labeled with pre- and postsynaptic markers. We expressed shRNA-LRP6 in dissociated neurons at 7 DIV and analyzed the number of excitatory and inhibitory synapses at 14 DIV using PSD95/VGluT1 and Gephyrin/VGAT immunostaining, respectively. Knockdown of LRP6 selectively reduced the number of excitatory synapses (Figure 2A, i–iv) and did not have any effect on inhibitory synapse number (Figure 2B). Reduction in excitatory synapse number was also reflected by a loss of spines as a result of LRP6 knockdown (Figure 2Av). The effect caused by the

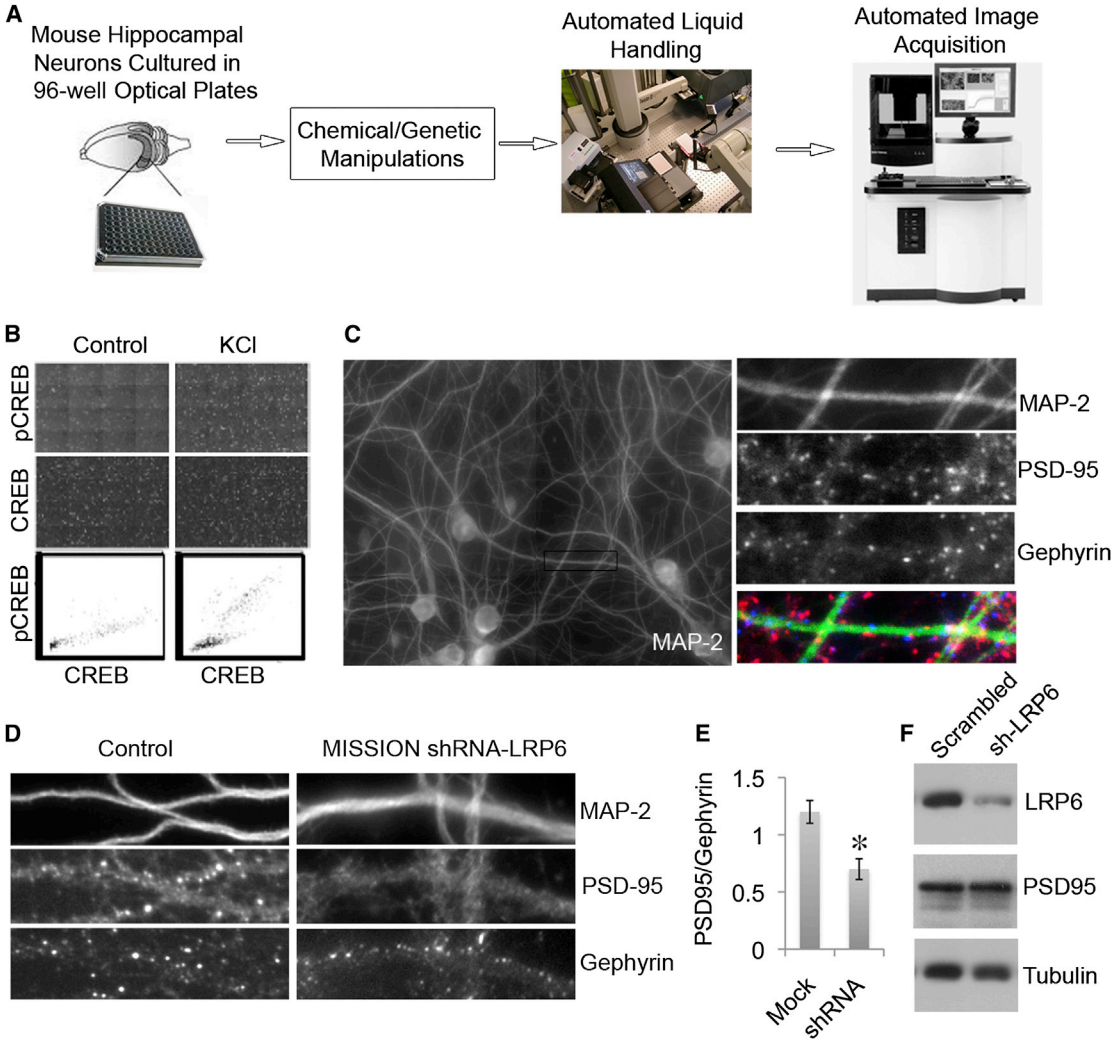

Figure 1. Strategy for High-Content Handling of Hippocampal Neurons

(A) Outline of high-content methodology.

(B) Neurons are physiologically responsive to changes in activity in the network as evident by enhanced phosphorylation of CREB in response to KCl-induced depolarization. Each dot in the pCREB/CREB signal plot represents signal intensity from phospho-CREB (pCREB) and total CREB antibodies. Panels where neurons were depolarized with KCl show a significant increase in the number of cells with higher pCREB signal intensity.

(C) Immunolabeling performed in an automated fashion is efficient and specific as shown by differential labeling with MAP-2, PSD95, and Gephyrin.

(D) One of the hits identified in the loss-of-function genetic screen is LRP6. Right panel shows a representative ROI from the well that received shRNA lentivirus against LRP6, and left panel shows ROI from the control well. shRNA-LRP6 led to reduction in PSD95 clustering in comparison to control.

(E) Quantification of a well that received shRNA-LRP6 shows a significant reduction in PSD95-to-Gephyrin puncta ratio (n = 30 ROIs from each well; $p < 0.05$, t test).

(F) shRNA-LRP6 that caused reduction in PSD95 clusters reduces levels of endogenous LRP6 protein significantly in neurons.

All error bars are SEM.

See also Figures S1 and S2.

shRNA could be rescued by shRNA-resistant human LRP6. In summary, we confirmed LRP6 as a bona fide hit in dissociated neuronal cultures that plays an important specific role in excitatory synapse development.

LRP6 Is Selectively Localized to Excitatory Synapses

To investigate the subcellular localization of endogenous LRP6, we immunostained dissociated neurons using LRP6 antibodies in conjunction with synaptic markers. First, we tested the specificity of antibodies in the neurons that were transiently transfected with shRNA-LRP6. We saw a significant reduction in LRP6 immunolabeling in neurons transfected with shRNA-LRP6 in comparison to neighboring untransfected neurons (Figure S3A). Specificity of the antibodies was also evident in western blot of total protein lysate from neurons electroporated with shRNA-LRP6 (Figure S3B). Next, in immunolocalization studies, LRP6 showed a punctate pattern with enrichment in spine heads. LRP6 was selectively colocalized with PSD95 and

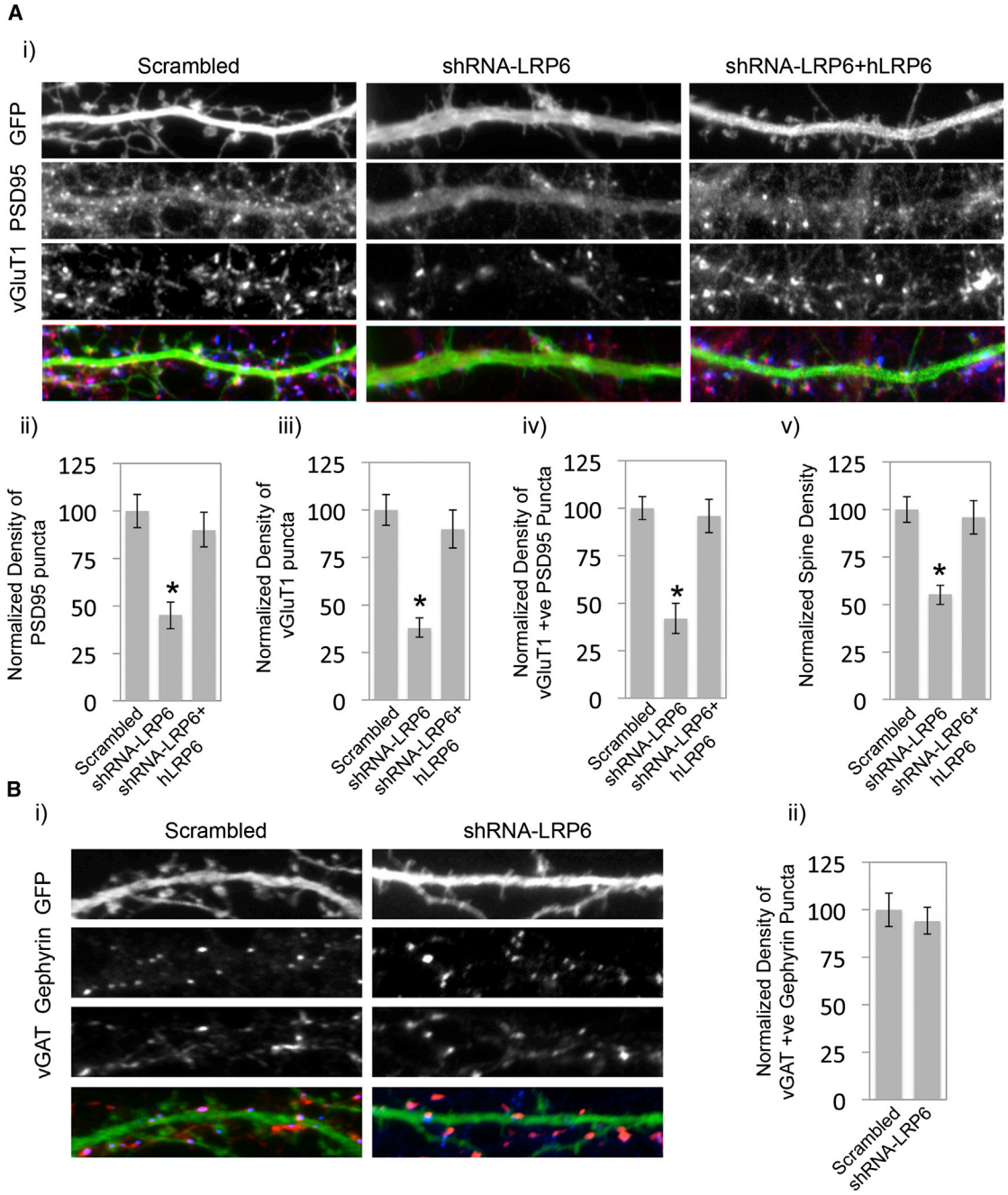

Figure 2. LRP6 Is Required Selectively for Excitatory Synaptogenesis

(A) (i–iv) The loss of LRP6 leads to reduction in excitatory synapses as evident by the reduced number of PSD95 and vGluT1 puncta (n = 20 each). Human LRP6 (hLRP6) that has sequence mismatch with shRNA against mouse/rat LRP6 can rescue the phenotype from effect of shRNA. (v) The loss of LRP6 causes reduction in spine density that can be rescued by hLRP6 (n = 20 each).

(B) (i and ii) Knockdown of LRP6 does not affect formation of inhibitory synapses because there was no change in the number of Gephyrin and vGAT puncta in neurons that were transfected with shRNA-LRP6 (n = 12; $p < 0.05$, t test).

Merged frames show GFP (green), PSD95 (red), and vGluT1 (blue) in (A), and GFP (green), Gephyrin (red), and vGAT (blue) in (B).

All error bars are SEM.

vGluT1 at excitatory synapses (Figure 3A). In contrast, LRP6 did not show significant colocalization with inhibitory postsynaptic marker Gephyrin (Figures 3B and 3C). To confirm the synaptic localization with an alternative biochemical method, we prepared PSD fractions and probed the samples with LRP6 antibodies. Supporting the immunostaining data, LRP6 showed

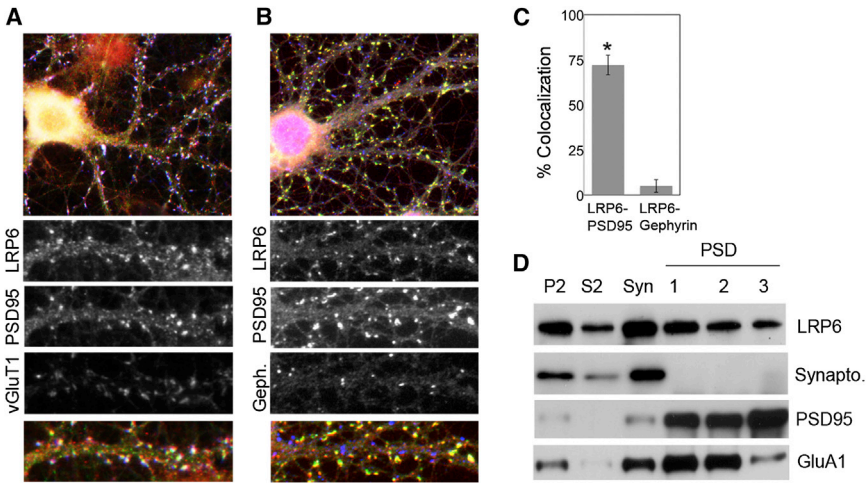

Figure 3. LRP6 Is Localized at Excitatory Synapses in Mature Neurons

(A) Immunolabeling of endogenous LRP6, PSD95, and presynaptic marker vGluT1 reveals that LRP6 is present at excitatory synapses.

(B) LRP6 does not show any significant level of colocalization with Gephyrin (Geph.), a postsynaptic marker for inhibitory synapses. Merged frames show LRP6 (red), PSD95 (green), and vGluT1/Gephyrin (blue).

(C) Quantification of overlap between LRP6 and PSD95 clusters in comparison to LRP6 and Gephyrin clusters reveals significant colocalization between LRP6 and PSD95, but not between LRP6 and Gephyrin ($n = 15$ each; $p < 0.001$, t test)

(D) In biochemical fractions of PSDs from mouse brain, endogenous LRP6 is detected in synaptosomal (Syn.) fractions including PSD fractions I, II, and III synaptic fractions. Synaptophysin (Synapto.) was used as a presynaptic marker for PSD samples.

All error bars are SEM.

See also Figure S3.

a pattern similar to that of PSD95 and GluA1 (Figure 3D) and was found to be a component of PSD fractions I, II, and III. Taken together, these results suggest that LRP6 is predominantly localized at excitatory synapses.

Wnt8A, a Ligand for LRP6, Promotes Excitatory Synapse Development

There are 19 Wnt ligands, few of which have been studied in the context of excitatory neurotransmission in the CNS. Wnt7a is the only well-characterized canonical Wnt ligand for its role in activity-dependent spine development and synapse formation in the mammalian CNS in vivo. However, expression analysis of different Wnts in the Allen Mouse Brain Atlas revealed that Wnt8A is expressed at relatively higher levels in comparison to other Wnt ligands in the forebrain area (Figure 4A; Lein et al. 2007). Although a functional interaction between Wnt8A and LRP6 has been described by Itasaki et al. (2003), the role of Wnt8a in synapse development is unknown.

First, to confirm the interaction between Wnt8A and LRP6, we tested if Wnt8A can associate with endogenous LRP6. HEK cells that have endogenous LRP6 were transfected with Wnt8A-myc cDNA. HEK cell lysate was subjected to immunoprecipitation with myc antibodies and probed for endogenous LRP6. In agreement with previous findings, we observed the pull down of endogenous LRP6 in Wnt8A-myc-transfected cells, but not in mock-transfected cells (data not shown).

Next, to determine whether Wnt8A has synaptogenic activity, neurons (11 DIV) were treated with conditioned media for 24 hr and analyzed for changes in synapse number. We observed that cultured neurons treated with Wnt8A condition media had an increased density of PSD95 and vGluT1 puncta but unchanged levels of Gephyrin puncta (Figures 4C and 4D), suggesting that Wnt8A specifically promotes formation and maturation of excitatory synapses. Next, we asked if LRP6 is required for the synaptogenic action of Wnt8A. To test this, we transfected neurons with shRNA against LRP6 and treated neurons with mock-conditioned media or Wnt8A-conditioned media. Confirming the role of LRP6 in synaptogenic action of Wnt8A, transfected neurons showed no increase in PSD95 and vGluT1 puncta (Figures 4E and 4F). Wnt8A potently increased the number of excitatory synapses in neurons transfected with scrambled shRNA (Figure S4). To investigate if Wnt8a is necessary for formation of excitatory synapses, we took a loss-of-function approach where we generated lentiviral particles carrying GFP and shRNA against Wnt8a. Neurons were infected with lentivirus on 4 DIV and tested for Wnt8A expression at 11 DIV. As shown in Figure S5A, we saw a significant reduction in Wnt8A levels in neuronal cultures. Next, we infected three sets of neuronal cultures at 4 DIV: one set was infected with control lentiviral particles, and two sets were infected with Wnt8A-targeting lentiviral particles. One of these two sets infected with Wnt8A-targeting lentiviral particles received Wnt8A-conditioned media every 24 hr from 10 to 14 DIV to compensate for the loss of endogenous Wnt8A. Neurons were fixed and immunostained at 14 DIV. We observed a significant decrease in the number of excitatory synapses in response to Wnt8A knockdown that could be rescued by exogenous application of Wnt8a (Figures S5B and S5C). Together, these data demonstrate that Wnt8a is necessary for formation of excitatory synapses, and it regulates excitatory synapse formation through LRP6.

Because LRP6 phosphorylation is one of the key events in the relay of Wnt signaling, we asked if Wnt8a could lead to changes in the phosphorylation status of LRP6. To test this, we prepared Wnt8A-conditioned media from Wnt8A-transfected HEK cells and control-conditioned media from mock-transfected HEK cells. Neurons were treated with Wnt8a-conditioned media for 3 hr, lysed, and probed with Phospho-LRP6 antibodies that recognized LRP6 phosphorylated at Serine residue (Tamai et al., 2004). We observed an increase in phosphorylation of LRP6 in response to Wnt8a treatment, suggesting a direct regulation of LRP6 phosphorylation by Wnt8a in neurons (Figures 5A and 5B). Next, we asked if LRP6 phosphorylation is one of the key steps required for synaptogenesis. To test this, we generated an LRP6 phosphomutant, LRP6S1490A, where

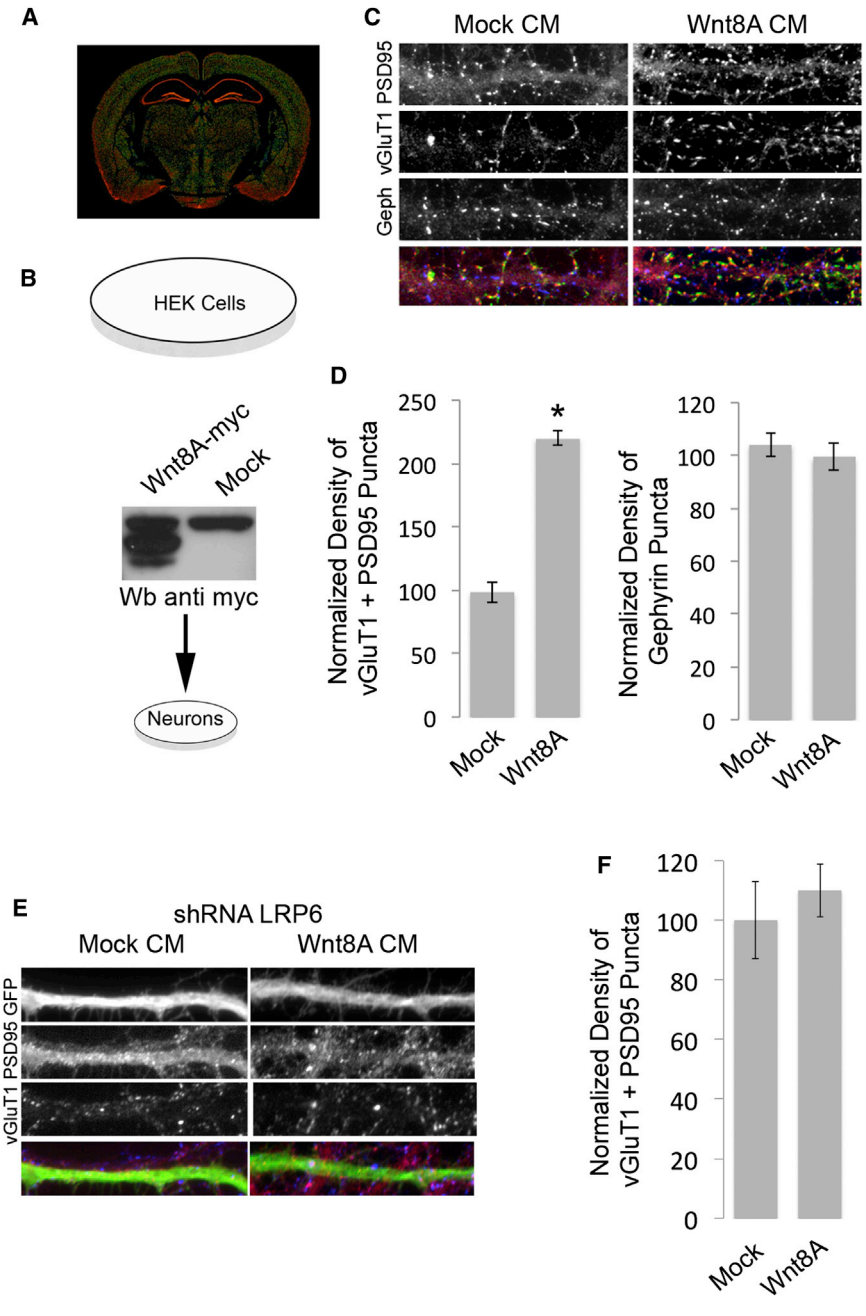

Figure 4. Wnt8A Induces Excitatory Synaptogenesis

(A) Wnt8A is significantly enriched in forebrain. Image is from the Allen Mouse Brain Atlas, Allen Institute for Brain Science; http://mouse.brain-map.org/gene/show/20652 (Lein et al. 2007).

(B) Wnt8A-conditioned media were prepared by overexpression of Wnt8A-myc in HEK cells. Neurons were treated with Wnt8A-conditioned media or mock-conditioned media for 24 hr. Wb, western blot.

(C) Neurons treated with Wnt8A show a significant increase in PSD95 and vGluT1 puncta, but no effect on Gephyrin puncta. CM, conditioned media.

(D) Quantification of PSD95, vGluT1, and Gephyrin puncta revealed a selective and significant increase in excitatory synapses ($n = 15$ each; $p < 0.005$, t test).

(E) shRNA-mediated knockdown of LRP6 diminishes the effect of Wnt8A.

(F) Quantification of vGLUT1-positive PSD95 puncta is shown.

Merged frames in (C) include PSD95 (red), vGluT1 (green), and Gephyrin (blue), and GFP (green), PSD95 (red), and vGluT1 (blue) in (E).

All error bars are SEM.

See also Figures S4 and S5.

LRP6 Is Required for Functional Synapse Development In Vivo

Studies in dissociated hippocampal neurons allow a wide range of manipulations and analysis at a higher resolution but have the limitation of belonging to a two-dimensional neuronal network system that may not truly recapitulate the complex development of three-dimensional brain architecture. To test if the role of LRP6 in synapse development observed in vitro holds true for the developing intact brain, and also if loss of LRP6 in fact leads to reduction in the number of functional synapses in vivo, we knocked down LRP6 in layer II/III cortical neurons by in utero electroporation of shRNA-LRP6 and dsRed at E15.5. Acute slices from animals at the age of postnatal day 21–28 (P21–P28) were prepared, and immunolabeled with antibodies against dsRed to analyze spine growth. Spines are the primary site for excitatory synapses and an accurate morphometric parameter to assess synapse density in vivo (Knott et al., 2006). Confirming in vitro results, we observed a significant reduction in the number of spines on the dendrites of layer II/III neurons in somatosensory cortex in animals expressing shRNA-LRP6 in comparison to the animals expressing scrambled shRNA (Figure 6). In addition, the effect on spine numbers caused by the shRNA-LRP6 could be rescued by shRNA-resistant human LRP6.

To test further if the reduction in spine number truly reflects a decrease in the number of functional synapses, we prepared

we replaced Serine-1490 with Alanine. As shown in Figure 5C, LRP6S1490A was targeted to dendritic spines in a fashion similar to that of wild-type LRP6. To determine if LRP6 phosphorylation is critical for synapse formation, we transfected neurons with an shRNA against LRP6 in conjunction with wild-type LRP6 or LRP6S1490A. Wild-type LRP6 efficiently rescued the loss of endogenous LRP6, but LRP6S1490A failed to rescue the effect of shRNA on synapse formation as well as on the formation of dendritic spines (Figures 5D and 5E). These results suggest that phosphorylation of LRP6 at Serine-1490 is crucial for the assembly of the synaptic apparatus.

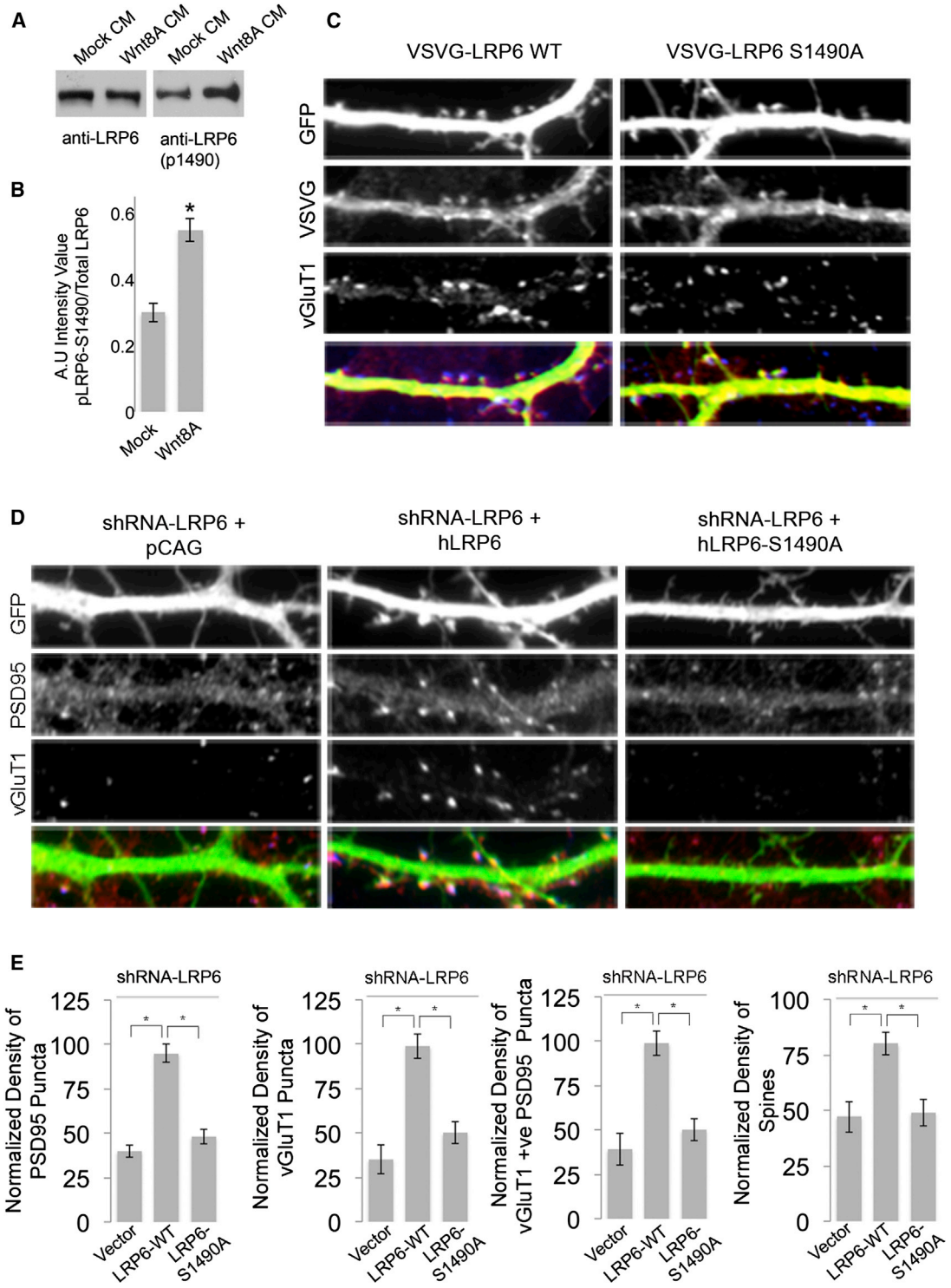

Figure 5. LRP6 Undergoes Wnt-Dependent Phosphorylation to Promote Synaptogenesis

(A and B) Wnt8A treatment leads to enhanced phosphorylation of LRP6.

(C) Transient transfection of VSVG-tagged LRP6 cDNA shows that LRP6S1490A is targeted to dendritic spine in a fashion similar to that of wild-type (WT) LRP6. Merged frame includes GFP (green), LRP6 and PSD95 (red), and vGluT1 (blue).

(D and E) Wild-type but not LRP6S1490A can rescue the effect of shRNA. Data in (E) were normalized to the average of the wild-type LRP6 rescue data set ($n = 14$ each; $p < 0.05$, t test).

All error bars are SEM.

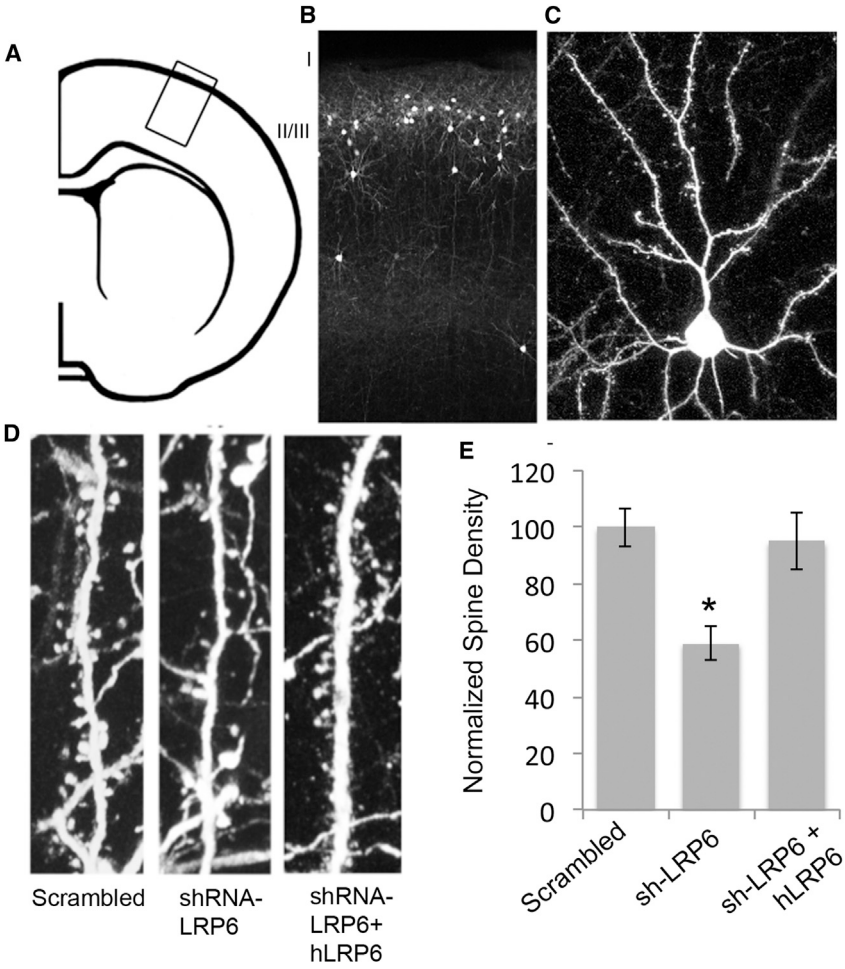

Figure 6. LRP6 Is Required for Spine Formation In Vivo

(A–C) In utero electroporation of shRNA and dsRed at the E15.5 stage result in efficient labeling of pyramidal neurons in layer II/III neurons in the somatosensory cortex of P28 animals.

(D and E) Neurons transfected with shRNA-LRP6 and dsRed have a significantly decreased number of spines in comparison to neurons transfected with scrambled shRNA and dsRed. This reduction in spine number is rescued by hLRP6 ($n = 12$; $p < 0.05$, t test).

All error bars are SEM.

slices from animals expressing either shRNA-LRP6 or scrambled shRNA and carried out analysis of miniature excitatory postsynaptic currents (mEPSCs). Further validating our earlier studies, we found that neurons expressing shRNA-LRP6 had a significant reduction in mEPSC frequency with relatively unchanged amplitude in comparison to neighboring untransfected neurons (Figure 7). In contrast, neurons expressing scrambled shRNA had no difference in frequency in comparison to neighboring untransfected neurons. Moreover, the effect caused by the shRNA-LRP6 could be rescued by shRNA-resistant human LRP6. Together, these results establish LRP6 as a bona fide hit of our screen that is critical for the development of functional excitatory synapses in vitro as well as in vivo.

DISCUSSION

We have optimized a high-throughput assay using primary neuronal cultures that can be employed for a diverse range of screening methods. With the exception of automated image analysis for complex synaptic patterns, we have carried out a loss-of-function screen to discover synaptogenic proteins in a fully automated manner. Traditionally, larger-scale screening has required the use of simpler culture systems. Hence, most screens are limited to nonneuronal cells or neuroblastoma cell lines (Jain and Heutink, 2010). The fragile nature of neurons and lack of versatile methods for gene delivery have posed significant challenges to the use of primary neuronal cultures in a high-throughput assay. Optimization of high-content culturing, genetic manipulations, immunostaining, and image acquisition of primary neuronal networks is the first major contribution of this work, and overcomes the conventional challenges of a larger screen requiring simpler cellular systems, to a significant extent. Notably, assays that have a simple readout parameter such as the ratio of total CREB to phosphorylated CREB fluorescent signal intensities (Figure 1), or expression of GFP or lack thereof, can be analyzed in high-throughput fashion enabling truly large-scale high-throughput screens in neurons. Reporter assays such as Wnt-regulated TCF/LEF can also be successfully employed in this platform to discover neuron-specific genetic components of the cascade or drug-like small molecule modulators of these pathways in neurons. This platform can be further optimized to discover regulators of activity-dependent protein trafficking, e.g., chemical LTP (long-term potentiation) paradigms can be employed in conjunction with surface labeling of AMPA receptor subunits. Recent advances in high-throughput electroporation of neurons have made it feasible to overexpress any given set of genes in 96-well formats, making it possible to carry out gain-of-function genetic screens using this platform.

The lack of reliable high-throughput image analysis tools to process images of mature neurons that have complex patterns of synaptic markers still remains a challenge and requires development. Typically, statistical parameters such as *Z* score and MAD scores provide indispensable tools to identify a hit and to calculate false discovery rate (Chung et al., 2008; König et al., 2007; Zhang et al., 1999). The limitation of currently available software to quantify synapse number with high stringency has forced us to manually inspect the wells, and select regions of interest (ROIs) for analysis. Computational tools available at present allow quantitative analysis of manually selected ROI

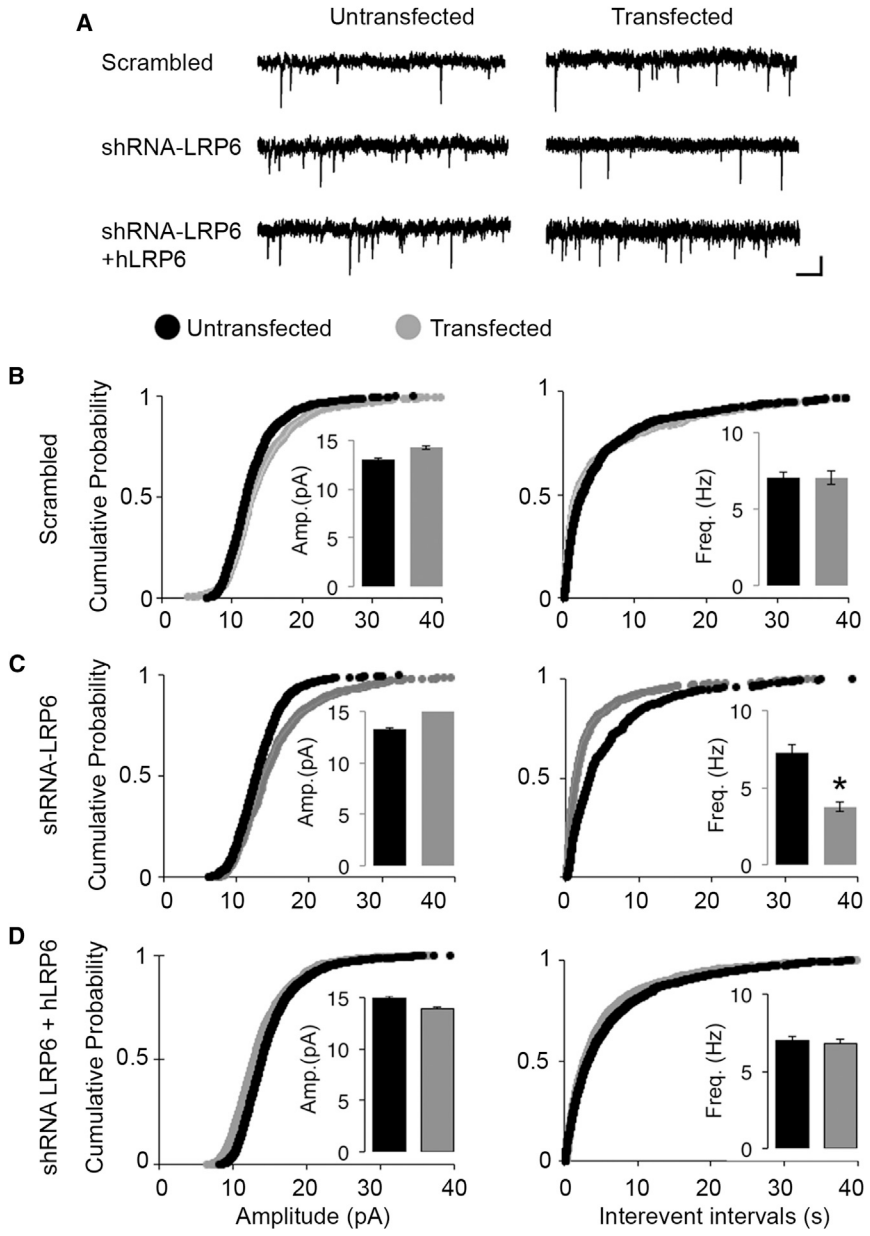

Figure 7. LRP6 Is Required for Formation of Functional AMPAR-Containing Synapses In Vivo

(A) Representative traces from neurons transfected with scrambled, shRNA-LRP6, or shRNA-LRP6+hLRP6 and neighboring untransfected neurons in corresponding group, in layer II/III neurons in somatosensory cortex, are shown. Scale is 200 ms at 10 pA.

(B) Neurons electroporated in utero with scrambled shRNA did not show any difference in mEPSC frequency (Freq.) in comparison to neighboring untransfected neurons (n = 8 each). Amp., amplitude.

(C) LRP6 knockdown led to a significant reduction in mEPSC frequency (n = 9 each; $p < 0.05$, t test). A small and nonsignificant increase was observed in mEPSC amplitude.

(D) Effect of shRNA against rat LRP6 can be rescued by hLRP6 (n = 15 control; n = 19 rescue). All error bars are SEM.

along the dendritic regions but fail to generate a quantitatively consistent readout when applied globally to images across the 96-well plates. The advancement of a computational tool to quantify synaptic labeling will significantly enhance the throughput of similar screens in the future. In summary, our system can be readily used for a wide variety of neuronal assays, and refinement of computational tools to analyze complex synaptic patterns will further enhance its capabilities.

One of the hits discovered in our loss-of-function shRNA screen is LRP6, a Wnt coreceptor. We present compelling data for a role for LRP6 in the development of functional excitatory synapses, and its direct association with the PSD in vivo. Furthermore, we show that a ligand for LRP6, Wnt8A, has synaptogenic activity. Given the complexity of Wnt signaling in mammals, it is important to understand the localization and role of each component of this signaling cascade. In contrast to invertebrates such as *Drosophila* or *C. elegans* that have 5 Wnt ligands and four Fzd receptors, Wnt signaling in mammals is comprised of 19 Wnt ligands and ten Fzd receptors (Ciani and Salinas, 2005). In recent years, elegant studies on the neuromuscular junction have paved the way to an understanding of Wnt signaling in synapse development (Korkut and Budnik, 2009). In mammals, different Wnt ligands have been shown to be important in axonal remodeling, dendritic growth (Wayman et al., 2006), synaptic development (Ciani et al., 2011; Gogolla et al., 2009; Varela-Nallar et al., 2010), and LTP (Chen et al., 2006). However, to date, no receptor member has been described to play a functional role in synapse development in the mammalian CNS in vivo. Despite a well-established canonical model in which LRP6 acts as an obligatory coreceptor for Fzd receptors, the role of LRP6 in synapse development and its localization has remained elusive. Here, we show that the key Wnt coreceptor LRP6 is predominantly present at excitatory synapses where it selectively regulates the development of functional excitatory synapses. These findings indicate either that canonical Wnt signaling is exclusively dedicated to excitatory synapses or that canonical Wnt signaling at excitatory and inhibitory synapses can employ a different suite of signaling receptors. Because noncanonical Wnt5A has been reported to play regulatory roles at excitatory and inhibitory synapses (Varela-Nallar et al., 2010), it is possible that a combination of canonical and noncanonical pathways regulates distinct synapse subtypes in forebrain. However, more experiments are required to draw a

distinction between the roles of different Wnts in the development of different synapse subtypes.

We also discovered Wnt8A as a synaptogenic factor that acts via its interaction with LRP6. A close analysis of different Wnt ligands for their localization in forebrain, and established interactions with LRP6, led us to investigate Wnt8A for its potential role in excitatory synaptogenesis. We found a role for Wnt8A that is specific to excitatory synapses. Wnt8A has been described as a canonical Wnt ligand that binds multiple Fzd receptors, and the Wnt8-Fzd complex further associates with LRP6 to transduce the signal. Interestingly, many of the Fzd receptors have PDZ binding motifs, and can bind to PSD95 (Hering and Sheng, 2002). This suggests a mechanism where Wnt8A triggers Wnt-Fzd-LRP6 complex formation and recruits intracellular signaling complex at the phosphorylated carboxyl terminus of LRP6 that can act further as a postsynaptic organizer. We have, in fact, discovered that Wnt8a triggers phosphorylation of LRP6 at Serine-1490. Our results further show that indeed phosphorylation of LRP6 is critical for synapse formation.

Our characterization of LRP6 suggests a specific role for canonical Wnt signaling in excitatory synapse development. It also raises many questions for future investigation. Most importantly, it will be necessary to identify which Fzd receptors associate with LRP6 to promote excitatory synapse development. Fzd receptors are the primary interaction partners for Wnt ligands and are shared between canonical and noncanonical Wnt ligands. It is possible that Fzd receptors have a widespread localization across excitatory and inhibitory synapses and that LRP6 confers specificity to canonical Wnt signaling pathways promoting excitatory synapse development and function. Based on this hypothesis, LRP6 may play a key role in balancing excitatory and inhibitory synaptic weights in neuronal networks. Besides regulating the development of different synapse subtypes, it is important to note that cyclin Y-dependent L63/PFTK kinase phosphorylates LRP6 in a ligand-independent manner during the cell cycle (Davidson et al., 2009). Interestingly, cyclin Y has been shown to dynamically regulate synapse elimination during network remodeling (Park et al., 2011). This suggests that LRP6 may not be only required for synaptogenesis but also may play a broader role in the context of activity-dependent remodeling at the network level independent of Wnt ligands. Our data provide a step forward in understanding the localization and function of a key Wnt receptor that acts as a hub for canonical Wnt signaling, as well as uncovering a role for another Wnt ligand. However, extensive and systematic studies are required to further decipher the combinatorial codes defined by Wnt-Fzd-LRP6 complexes that act in a context-dependent manner. Our optimized platform for high-throughput assay to study synapse development can play an important role in delineating signaling cascades under a given set of parameters in the future.

EXPERIMENTAL PROCEDURES

Animal Care

All animals were treated in accordance with the Johns Hopkins University Animal Care and Use Committee guidelines.

cDNA and Antibodies

LRP6 cDNA was obtained from Addgene (Addgene plasmid 27242) (Tamai et al., 2000). ORF was amplified and subcloned into pCAG plasmid. Phosphomutant LRP6S1490A was generated by using QuikChange Site-Directed Mutagenesis Kit from Stratagene. *Wnt8a* cDNA was obtained from Addgene (Addgene plasmid 35916) (Najdi et al., 2012) and amplified to subclone into pCDNA3.1-Myc plasmid.

The following antibodies (and resources) were used in this study: PSD95 K28/43 (NeuroMabs; 1:2,500); Gephyrin IgG1 (Synaptic Systems; 0.5 μg/ml); vGluT1 guinea pig (Millipore; 1:5,000); vGAT rabbit polyclonal (Synaptic Systems; 1:1,000); MAP-2 chicken (Novus Biologicals; 1:20,000); LRP6 C5C7 (Cell Signaling Technology; 1:2,500 for western blot only); LRP6 rabbit monoclonal (Epitomics; 1:2,000 for western blot and 1:500 for immunocytochemistry); and LRP6-pS1490 (Cell Signaling Technology; 1:1,000 for western blot). All the primary antibodies were incubated at 4°C overnight. Secondary antibodies were conjugated with Alexa Fluor dyes and used at 1:500 dilutions.

Neuronal Cultures and Immunocytochemistry

Primary hippocampal neurons were prepared from mouse or rat as described elsewhere by Brewer and Cotman (1989). In brief, for high-throughput assays, neurons were dissociated from E16.5 mouse or E18 rat hippocampi and plated into 96-well optical plates using the multidrop apparatus (Thermo Scientific). For high-content assays, mouse neurons were plated at the density of 10,000 neurons per well, and rat neurons were plated at 6,000 neurons per well. Neurons were maintained at 37°C in a 5% CO_2 incubator. Half of the media were changed every fourth day. A similar protocol was followed for small-scale culturing in 12-well plates on poly-L-lysine-coated coverslips. For automated immunolabeling, a multidrop plate washer and a robotic arm were employed using optimized programs. After the last step of washing, neurons were preserved in fixation solution.

CREB Phosphorylation Assay

Rat neurons from E18 embryos were used for a pilot chemical screen to identify small molecules that can modulate CREB pathway. On 14 DIV, neurons were treated with Sigma-Aldrich LOPAC chemical library compounds for 1 hr at a final concentration of 10 μM. Neurons were depolarized with 50 mM KCl in artificial cerebrospinal fluid (ACSF) for 20 min. Neurons were fixed and immunostained with antibodies against CREB and Phospho-CREB. Images were acquired as described above.

Image Acquisition and Analysis

High-content image acquisition was carried out at BD Pathway Imaging Station. Images were acquired using a 40× objective in 4 × 4 montage format that covered a network of 25–35 neurons per well. Wells that showed obvious reduction in puncta count were analyzed by using ImageJ where ROIs were selected on the basis on MAP2 staining and overlapped with PSD95 and Gephyrin-labeled images. After background subtraction and thresholding, puncta were counted using Analyze Particle tool.

For the validation step, ROIs were selected on the basis of GFP expression and analyzed as described above. The length of the dendrite was measured using NeuronJ plugin. The data were normalized to the average of the control group and plotted as the percentage of the average of the control.

ShRNA Loss-of-Function Genetic Screen

Mouse neurons prepared from E16.5 embryos were used for a loss-of-function genetic screen. Lentiviral particle suspension from the MISSION shRNA Library was used at 10,000 TU/ml to infect neurons at 4 DIV. Neurons were fixed and immunostained at 13 DIV for somatodendritic marker MAP2, and synaptic markers PSD95 and Gephyrin. Images were acquired by a BD Pathway Imaging Station microscope in laser-autofocus mode in 4 × 4 montages per well. For follow-up studies, LRP6 was knocked down in dissociated neurons with shRNA (5′-CGCACTACATTAGTTCCAAA-3′) that has common target in rat and mouse but not in human *LRP6*. Effect of shRNA was rescued by human LRP6.

In Utero Electroporation and Immunohistochemistry

In utero electroporation was carried out as described by Tabata and Nakajima (2001). In brief, uterine horns of E15.5 mice were surgically exposed under

anesthesia, and ~3 μg DNA mixed with fast green was injected into lateral ventricles. DNA was electroporated with five pulses at 950 ms intervals at 40 V for 50 ms with a tweezers electrode. Embryos were then placed back, and the abdominal wall was sutured. At P28, mice were perfused with PBS followed by 4% paraformaldehyde in PBS. Brains were fixed for 24 hr followed by cryoprotection by 30% sucrose in PBS. One hundred fifty-micrometer-thick slices were cut in coronal plane with a vibratome and immunostained with dsRed antibodies. Optical sections in Z planes were acquired using the Zeis 510 laser-scanning confocal microscope.

Electrophysiology

Three- to 5-week-old in utero-electroporated mice were anesthetized by isoflurane inhalation and decapitated. Brains were quickly dissected in ice-cold buffer (212.7 mM sucrose, 10 mM glucose, 2.6 mM KCl, 1.23 mM NaH_2PO_4, 26 mM $NaHCO_3$, 0.5 mM $CaCl_2$, and 5 mM $MgCl_2$). Brains were sliced into 300 μm thin slices with a vibratome in the same solution and transferred to normal ACSF (124 mM NaCl, 5 mM KCl, 1.23 mM NaH_2PO_4, 26 mM $NaHCO_3$, 10 mM glucose, 2 mM $CaCl_2$, and 1 mM $MgCl_2$). Slices were allowed to recover for 1 hr at 30°C and maintained at room temperature (22°C–25°C). Neurons were targeted for whole-cell patch-clamp recording with borosilicate glass electrodes of 3–6 MΩ resistance. The electrode internal solution consisted of 130 mM cesium methanesulphonate, 10 mM HEPES, 0.5 mM EGTA, 8 mM CsCl, 5 mM TEA-Cl, 1 mM QX-314, 10 mM Na phosphocreatine, 0.5 mM Na-GTP, and 4 mM Na-ATP. Cortical pyramidal neurons with or without fluorescence were selected from layers II–V of primary somatosensory cortex through entorhinal cortex. For AMPA receptor-mediated mEPSCs, external solution was supplemented with 1 μM tetrodotoxin, 50 μM d,l-APV (2-amino-5-phosphonovalerate), and 100 μM picrotoxin. Data were acquired with a MultiClamp 700A, and Clampex 8 program (Molecular Devices), at 10 kHz. Current traces were low-pass filtered at 1 kHz prior to mEPSC detection and analysis. mEPSCs were detected and analyzed using Mini Analysis (Synaptosoft) or Clampfit 10 program (Molecular Devices).

SUPPLEMENTAL INFORMATION

Supplemental Information includes five figures and can be found with this article online at http://dx.doi.org/10.1016/j.celrep.2013.11.008.

ACKNOWLEDGMENTS

This work was supported by grants from the Howard Hughes Medical Institute (to R.L.H.) and the National Institutes of Health (5U54MH084691 to M.L.). Under a licensing agreement between Millipore Corporation and The Johns Hopkins University, R.L.H. is entitled to a share of royalties received by the University on sales of products described in this article. R.L.H. is a paid consultant to Millipore Corporation. The terms of this arrangement are being managed by The Johns Hopkins University in accordance with its conflict-of-interest policies.

Received: January 23, 2013
Revised: September 30, 2013
Accepted: November 4, 2013
Published: December 5, 2013

REFERENCES

Aberle, H., Haghighi, A.P., Fetter, R.D., McCabe, B.D., Magalhães, T.R., and Goodman, C.S. (2002). wishful thinking encodes a BMP type II receptor that regulates synaptic growth in *Drosophila*. Neuron *33*, 545–558.

Allen, N.J., Bennett, M.L., Foo, L.C., Wang, G.X., Chakraborty, C., Smith, S.J., and Barres, B.A. (2012). Astrocyte glypicans 4 and 6 promote formation of excitatory synapses via GluA1 AMPA receptors. Nature *486*, 410–414.

Brewer, G.J., and Cotman, C.W. (1989). Survival and growth of hippocampal neurons in defined medium at low density: advantages of a sandwich culture technique or low oxygen. Brain Res. *494*, 65–74.

Chen, J., Park, C.S., and Tang, S.J. (2006). Activity-dependent synaptic Wnt release regulates hippocampal long term potentiation. J. Biol. Chem. *281*, 11910–11916.

Chih, B., Engelman, H., and Scheiffele, P. (2005). Control of excitatory and inhibitory synapse formation by neuroligins. Science *307*, 1324–1328.

Christopherson, K.S., Ullian, E.M., Stokes, C.C., Mullowney, C.E., Hell, J.W., Agah, A., Lawler, J., Mosher, D.F., Bornstein, P., and Barres, B.A. (2005). Thrombospondins are astrocyte-secreted proteins that promote CNS synaptogenesis. Cell *120*, 421–433.

Chung, N., Zhang, X.D., Kreamer, A., Locco, L., Kuan, P.F., Bartz, S., Linsley, P.S., Ferrer, M., and Strulovici, B. (2008). Median absolute deviation to improve hit selection for genome-scale RNAi screens. J. Biomol. Screen. *13*, 149–158.

Ciani, L., and Salinas, P.C. (2005). WNTs in the vertebrate nervous system: from patterning to neuronal connectivity. Nat. Rev. Neurosci. *6*, 351–362.

Ciani, L., Boyle, K.A., Dickins, E., Sahores, M., Anane, D., Lopes, D.M., Gibb, A.J., and Salinas, P.C. (2011). Wnt7a signaling promotes dendritic spine growth and synaptic strength through Ca^{2+}/Calmodulin-dependent protein kinase II. Proc. Natl. Acad. Sci. USA *108*, 10732–10737.

Dalva, M.B., Takasu, M.A., Lin, M.Z., Shamah, S.M., Hu, L., Gale, N.W., and Greenberg, M.E. (2000). EphB receptors interact with NMDA receptors and regulate excitatory synapse formation. Cell *103*, 945–956.

Davidson, G., Shen, J., Huang, Y.L., Su, Y., Karaulanov, E., Bartscherer, K., Hassler, C., Stannek, P., Boutros, M., and Niehrs, C. (2009). Cell cycle control of wnt receptor activation. Dev. Cell *17*, 788–799.

Featherstone, D.E., Rushton, E.M., Hilderbrand-Chae, M., Phillips, A.M., Jackson, F.R., and Broadie, K. (2000). Presynaptic glutamic acid decarboxylase is required for induction of the postsynaptic receptor field at a glutamatergic synapse. Neuron *27*, 71–84.

Garner, C.C., Nash, J., and Huganir, R.L. (2000). PDZ domains in synapse assembly and signalling. Trends Cell Biol. *10*, 274–280.

Gogolla, N., Galimberti, I., Deguchi, Y., and Caroni, P. (2009). Wnt signaling mediates experience-related regulation of synapse numbers and mossy fiber connectivities in the adult hippocampus. Neuron *62*, 510–525.

Graf, E.R., Zhang, X., Jin, S.X., Linhoff, M.W., and Craig, A.M. (2004). Neurexins induce differentiation of GABA and glutamate postsynaptic specializations via neuroligins. Cell *119*, 1013–1026.

Hering, H., and Sheng, M. (2002). Direct interaction of Frizzled-1, -2, -4, and -7 with PDZ domains of PSD-95. FEBS Lett. *521*, 185–189.

Itasaki, N., Jones, C.M., Mercurio, S., Rowe, A., Domingos, P.M., Smith, J.C., and Krumlauf, R. (2003). Wise, a context-dependent activator and inhibitor of Wnt signalling. Development *130*, 4295–4305.

Jain, S., and Heutink, P. (2010). From single genes to gene networks: high-throughput-high-content screening for neurological disease. Neuron *68*, 207–217.

Knott, G.W., Holtmaat, A., Wilbrecht, L., Welker, E., and Svoboda, K. (2006). Spine growth precedes synapse formation in the adult neocortex in vivo. Nat. Neurosci. *9*, 1117–1124.

Koles, K., and Budnik, V. (2012). Wnt signaling in neuromuscular junction development. Cold Spring Harb. Perspect. Biol. *4*, a008045.

König, R., Chiang, C.Y., Tu, B.P., Yan, S.F., DeJesus, P.D., Romero, A., Bergauer, T., Orth, A., Krueger, U., Zhou, Y., and Chanda, S.K. (2007). A probability-based approach for the analysis of large-scale RNAi screens. Nat. Methods *4*, 847–849.

Korkut, C., and Budnik, V. (2009). WNTs tune up the neuromuscular junction. Nat. Rev. Neurosci. *10*, 627–634.

Kurusu, M., Cording, A., Taniguchi, M., Menon, K., Suzuki, E., and Zinn, K. (2008). A screen of cell-surface molecules identifies leucine-rich repeat proteins as key mediators of synaptic target selection. Neuron *59*, 972–985.

Lein, E.S., Hawrylycz, M.J., Ao, N., Ayres, M., Bensinger, A., Bernard, A., Boe, A.F., Boguski, M.S., Brockway, K.S., Byrnes, E.J., et al. (2007). Genome-wide atlas of gene expression in the adult mouse brain. Nature *445*, 168–176.

Linhoff, M.W., Laurén, J., Cassidy, R.M., Dobie, F.A., Takahashi, H., Nygaard, H.B., Airaksinen, M.S., Strittmatter, S.M., and Craig, A.M. (2009). An unbiased expression screen for synaptogenic proteins identifies the LRRTM protein family as synaptic organizers. Neuron *61*, 734–749.

McAllister, A.K. (2007). Dynamic aspects of CNS synapse formation. Annu. Rev. Neurosci. *30*, 425–450.

Melom, J.E., and Littleton, J.T. (2011). Synapse development in health and disease. Curr. Opin. Genet. Dev. *21*, 256–261.

Miech, C., Pauer, H.U., He, X., and Schwarz, T.L. (2008). Presynaptic local signaling by a canonical wingless pathway regulates development of the *Drosophila* neuromuscular junction. J. Neurosc. *28*, 10875–10884.

Mitchell, K.J. (2011). The genetics of neurodevelopmental disease. Curr. Opin. Neurobiol. *21*, 197–203.

Najdi, R., Proffitt, K., Sprowl, S., Kaur, S., Yu, J., Covey, T.M., Virshup, D.M., and Waterman, M.L. (2012). A uniform human Wnt expression library reveals a shared secretory pathway and unique signaling activities. Differentiation *84*, 203–213.

Nitkin, R.M., Smith, M.A., Magill, C., Fallon, J.R., Yao, Y.M., Wallace, B.G., and McMahan, U.J. (1987). Identification of agrin, a synaptic organizing protein from Torpedo electric organ. J. Cell Biol. *105*, 2471–2478.

Okabe, S. (2012). Molecular dynamics of the excitatory synapse. Adv. Exp. Med. Biol. *970*, 131–152.

O'Rourke, N.A., Weiler, N.C., Micheva, K.D., and Smith, S.J. (2012). Deep molecular diversity of mammalian synapses: why it matters and how to measure it. Nat. Rev. Neurosci. *13*, 365–379.

Packard, M., Koo, E.S., Gorczyca, M., Sharpe, J., Cumberledge, S., and Budnik, V. (2002). The *Drosophila* Wnt, wingless, provides an essential signal for pre- and postsynaptic differentiation. Cell *111*, 319–330.

Paradis, S., Harrar, D.B., Lin, Y., Koon, A.C., Hauser, J.L., Griffith, E.C., Zhu, L., Brass, L.F., Chen, C., and Greenberg, M.E. (2007). An RNAi-based approach identifies molecules required for glutamatergic and GABAergic synapse development. Neuron *53*, 217–232.

Park, M., Watanabe, S., Poon, V.Y., Ou, C.Y., Jorgensen, E.M., and Shen, K. (2011). CYY-1/cyclin Y and CDK-5 differentially regulate synapse elimination and formation for rewiring neural circuits. Neuron *70*, 742–757.

Peng, H.B., Baker, L.P., and Chen, Q. (1991). Induction of synaptic development in cultured muscle cells by basic fibroblast growth factor. Neuron *6*, 237–246.

Penzes, P., Beeser, A., Chernoff, J., Schiller, M.R., Eipper, B.A., Mains, R.E., and Huganir, R.L. (2003). Rapid induction of dendritic spine morphogenesis by trans-synaptic ephrinB-EphB receptor activation of the Rho-GEF kalirin. Neuron *37*, 263–274.

Pinson, K.I., Brennan, J., Monkley, S., Avery, B.J., and Skarnes, W.C. (2000). An LDL-receptor-related protein mediates Wnt signalling in mice. Nature *407*, 535–538.

Schaefer, A.M., Hadwiger, G.D., and Nonet, M.L. (2000). rpm-1, a conserved neuronal gene that regulates targeting and synaptogenesis in *C. elegans*. Neuron *26*, 345–356.

Scheiffele, P., Fan, J., Choih, J., Fetter, R., and Serafini, T. (2000). Neuroligin expressed in nonneuronal cells triggers presynaptic development in contacting axons. Cell *101*, 657–669.

Shen, K., and Scheiffele, P. (2010). Genetics and cell biology of building specific synaptic connectivity. Annu. Rev. Neurosci. *33*, 473–507.

Sheng, M., McFadden, G., and Greenberg, M.E. (1990). Membrane depolarization and calcium induce c-fos transcription via phosphorylation of transcription factor CREB. Neuron *4*, 571–582.

Siddiqui, T.J., and Craig, A.M. (2011). Synaptic organizing complexes. Curr. Opin. Neurobiol. *21*, 132–143.

Tabata, H., and Nakajima, K. (2001). Efficient in utero gene transfer system to the developing mouse brain using electroporation: visualization of neuronal migration in the developing cortex. Neuroscience *103*, 865–872.

Takahashi, H., Arstikaitis, P., Prasad, T., Bartlett, T.E., Wang, Y.T., Murphy, T.H., and Craig, A.M. (2011). Postsynaptic TrkC and presynaptic PTPσ function as a bidirectional excitatory synaptic organizing complex. Neuron *69*, 287–303.

Tamai, K., Semenov, M., Kato, Y., Spokony, R., Liu, C., Katsuyama, Y., Hess, F., Saint-Jeannet, J.P., and He, X. (2000). LDL-receptor-related proteins in Wnt signal transduction. Nature *407*, 530–535.

Tamai, K., Zeng, X., Liu, C., Zhang, X., Harada, Y., Chang, Z., and He, X. (2004). A mechanism for Wnt coreceptor activation. Mol. Cell *13*, 149–156.

van Amerongen, R., Mikels, A., and Nusse, R. (2008). Alternative wnt signaling is initiated by distinct receptors. Sci. Signal. *1*, re9.

Varela-Nallar, L., Alfaro, I.E., Serrano, F.G., Parodi, J., and Inestrosa, N.C. (2010). Wingless-type family member 5A (Wnt-5a) stimulates synaptic differentiation and function of glutamatergic synapses. Proc. Natl. Acad. Sci. USA *107*, 21164–21169.

Wayman, G.A., Impey, S., Marks, D., Saneyoshi, T., Grant, W.F., Derkach, V., and Soderling, T.R. (2006). Activity-dependent dendritic arborization mediated by CaM-kinase I activation and enhanced CREB-dependent transcription of Wnt-2. Neuron *50*, 897–909.

Wehrli, M., Dougan, S.T., Caldwell, K., O'Keefe, L., Schwartz, S., Vaizel-Ohayon, D., Schejter, E., Tomlinson, A., and DiNardo, S. (2000). arrow encodes an LDL-receptor-related protein essential for Wingless signalling. Nature *407*, 527–530.

Williams, M.E., de Wit, J., and Ghosh, A. (2010). Molecular mechanisms of synaptic specificity in developing neural circuits. Neuron *68*, 9–18.

Zhang, J.H., Chung, T.D., and Oldenburg, K.R. (1999). A simple statistical parameter for use in evaluation and validation of high throughput screening assays. J. Biomol. Screen. *4*, 67–73.